Colloids and Surfaces B: Biointerfaces 82 (2011) 168–172

Contents lists available at ScienceDirect

Colloids and Surfaces B: Biointerfaces

journal homepage: www.elsevier.com/locate/colsurfb

Improved glucose electrochemical biosensor by appropriate immobilization of nano-ZnO

Yang Lei [a], Xiaoqin Yan [a], Jing Zhao [a], Xi Liu [b], Yu Song [a], Ning Luo [a], Yue Zhang [a,b,*]

[a] State Key Laboratory for Advanced Metals and Materials, School of Materials Science & Engineering, University of Science & Technology Beijing 100083, PR China
[b] Key Laboratory of New Energy Materials and Technologies, University of Science & Technology Beijing 100083, PR China

ARTICLE INFO

Article history:
Received 20 May 2010
Received in revised form 15 July 2010
Accepted 22 August 2010
Available online 16 September 2010

Keywords:
ZnO nanorod
Biosensor
Glucose oxidase
Electrochemistry

ABSTRACT

We constructed the transferred ZnO biosensor and the grown ZnO biosensor by two different nano-ZnO immobilization approaches. And the influence of different assembly processes on the biosensor performance has been systematically investigated and compared. An enhanced sensitivity of the grown ZnO biosensor is found to be 52% higher than that of the transferred ZnO biosensor. Correspondingly, the other properties are also better in the grown ZnO biosensor, including the response time, the detection limit and the linear range. These results are well consistent with the fact that more glucose oxidase is immobilized on the well-aligned ZnO arrays, which have higher specific surface area and more direct electron communication path, in the grown sensor than the randomly distributed and stacked ZnO nanorods in the transferred sensor. The nano-ZnO grown directly has been demonstrated more desirable for enzymatic immobilization and signal transduction in the high performance biosensors.

1. Introduction

ZnO is an attractive semiconductor material with wide direct band gap (3.37 eV at room temperature), large exciton binding energy (60 meV) and a hexagonal structure, and have significant applications in optics, optoelectronics, sensors, and actuators [1,2]. Additionally, ZnO is also a biocompatible material with a high isoelectric point (IEP) of about 9.5, which make it suitable for absorption of low IEP proteins such as glucose oxidase (GO_x, IEP ~4.2), as the protein immobilization is primarily driven by electrostatic interaction [3]. Hence, ZnO is one of the most desirable platforms for binding enzyme and a promising material for a wide range of biosensor applications.

Notably, quasi one-dimensional (1D) ZnO nanostructures possess unique properties of high specific surface area, nontoxicity, chemical stability, electrochemical activity and high electron communication features [4]. Recently, quasi 1D nanostructured ZnO has been widely investigated and developed in the biological field, especially to be utilized as enzyme-modified biosensors to improve their sensitivity and the limit of detection (LOD) as compared to those prepared from bulk and thin film forms of ZnO [5–7]. For instance, Wang et al. first used quasi 1D ZnO nanostructures, nanocombs, as supporting materials for electrochemical biosensors with a high affinity of GO_x to glucose [8]. Wei et al. fabricated the glucose biosensor by ZnO nanorod arrays directly grown on electrodes without coated Nafion solution [9]. In our group, quasi 1D ZnO nanotetrapods were first utilized to construct the biosensors with high sensitivity to glucose, and we have proved nanostructural ZnO morphology is one of the important factors determining the properties [10].

More recently, some bioelectrodes using 1D ZnO nanomaterials have been realized to detect glucose [11], hydrogen peroxide (H_2O_2) [12], phenol [13], cholesterol [14] and so on. And the enzymic immobilization is employed by various conventional methods, such as physical adsorption [15], cross-linking [16], self-assembly [17], polymers [18], and sol–gels [19], etc. However, previous studies ignored the techniques of ZnO immobilization on the standard electrodes and the corresponding impact on the biosensor performance. In this work, we shall report comparative studies of the performance of two kinds of ZnO nanorod biosensors for glucose detection. We constructed the different biosensors through transferring the ZnO nanorod powder and preparing the ZnO nanorod arrays directly on the gold electrode, respectively. An enhanced sensitivity of the grown ZnO biosensor as compared to the transferred ZnO biosensor is reported.

2. Experimental details

The ZnO immobilization was achieved by covering the electrode surface with ZnO nanorods powder (Coating Method) and growing

* Corresponding author at: State Key Laboratory for Advanced Metals and Materials, School of Materials Science & Engineering, University of Science & Technology Beijing 100083, PR China. Tel.: +86 10 62334725; fax: +86 10 62333113.
E-mail address: yuezhang@ustb.edu.cn (Y. Zhang).

0927-7765/$ – see front matter © 2010 Elsevier B.V. All rights reserved.
doi:10.1016/j.colsurfb.2010.08.034

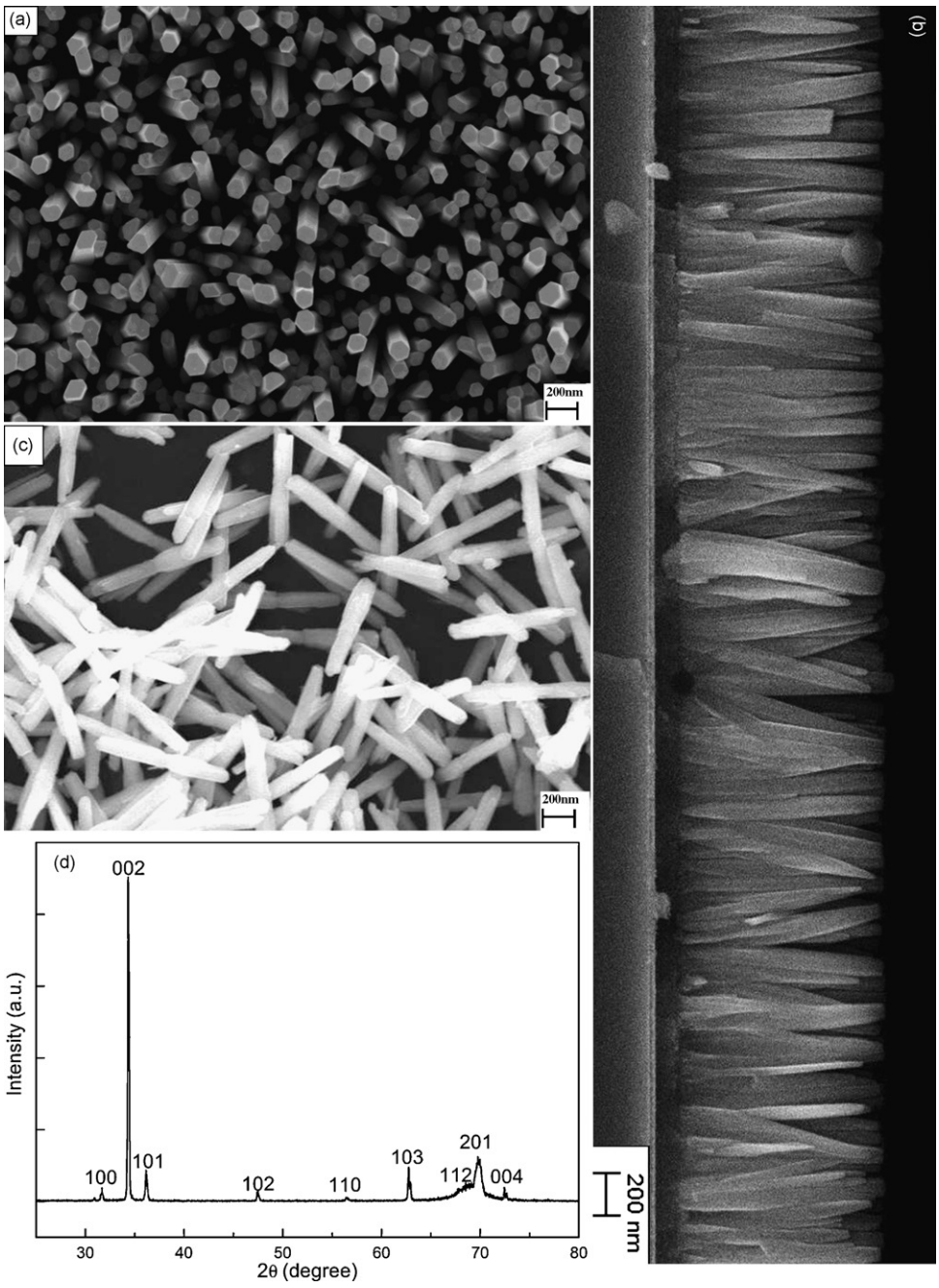

Fig. 1. FESEM images of as-grown nano-ZnO. (a) Top view, (b) side view of the ZnO arrays grown directly and (c) the transferred ZnO nanorods. (d) Typical XRD pattern of ZnO nanorods. A weak peak overlapped with (1 1 2) peak is from the Si substrate.

on the electrode surface directly (Growth Method), respectively. Method 1 was as follows. ZnO nanorods were synthesized by the hydrothermal decomposition method on Si substrates in a large scale. The reaction solution was prepared by mixing proper quantity of 0.05 M $Zn(NO_3)_2$ and methenamine ($(CH_2)_6N_4$) solutions in a Teflon-lined autoclave [20]. The desirable reaction conditions are 95 °C and 7 h. The white colored powder collected from Si wafers, wetted by 0.01 M phosphate buffer solution (PBS) with pH 7.4, were coated onto the surface of a Au electrode, and then dried after being compacted [10]. On the other hand, ZnO nanorod arrays were grown on the polished gold wires directly via the similar hydrothermal method. The gold electrode was horizontally immersed in the reaction solution, and then a layer of white products on the gold wires was obtained after the reaction. Both ZnO/Au electrodes were thoroughly washed with PBS and dried in air. After the ZnO immobilization, 5 μL GO_x (10 mg/mL, 100 units/mg) and 10 μL Nafion (5 wt.%) solutions were attached to the surface of ZnO/Au electrodes, successively. Then the modified electrodes were kept at 4 °C overnight followed by rinsing carefully to remove the loosely bound GO_x. Finally, the bioelectrodes were ready for further characterization. The morphologies of pure ZnO and functionalized ZnO nanostructures were characterized by field emission scanning electron microscope (FESEM). X-ray diffraction (XRD) and Energy dispersive X-ray spectra (EDX) were designed to examine the crystal structures and composition of two types of the samples.

The electrochemical and glucose sensing experiments were performed with two kinds of different ZnO bioelectrodes by taking a three-electrode system commonly used in electrochemistry. The system consisted of the ZnO modified working electrode, a Pt wire as counter electrode, and an Ag/AgCl reference electrode.

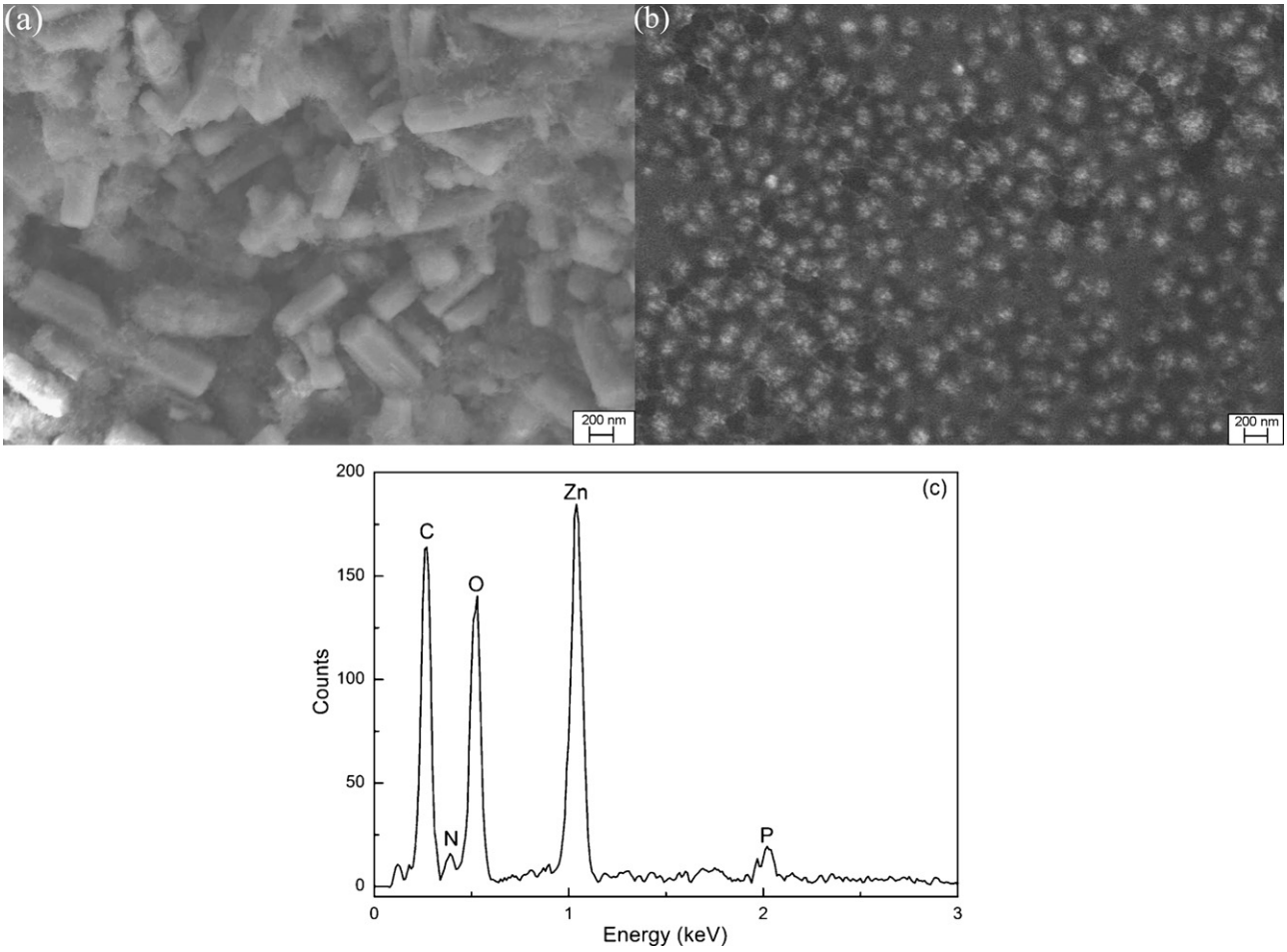

Fig. 2. FESEM micrographs of GO_x functionalized surface of (a) the transferred ZnO nanorods and (b) the grown arrays and (c) the typical EDX spectrum.

Cyclic voltammetric (CV) measurements were carried out in 30 mL unstirred 0.01 M PBS ranging from −0.2 to +0.8 V at a scan rate of 50 mV/s. For the glucose detection, the ZnO bioelectrodes were inserted in continuously stirred (500 rpm) solutions with different glucose concentrations, using a magnetic stirrer to have sufficient convective transport. A 10 μL glucose solution was added in each step using a micro-liter pipette at 0.8 V. All the measurements were performed at room temperature and all the potentials mentioned above were versus Ag/AgCl electrode.

3. Results and discussion

Fig. 1(a–c) show the FESEM micrographs of ZnO nanorods used for bio-sensing. The vertical nanorod arrays grown on the Au wires surface directly are found to be uniformly distributed with an average diameter of around 100 nm and well-aligned in a hexagonal structure morphology (a and b). The length of nanorods is about 1 μm and the aspect ratio is estimated to be upon 10. As the materials of the other biosensor, the white ZnO nanorod powder, which was collected from the Si substrate and transferred onto the electrodes, is shown in Fig. 1(c). It can be seen that the nanorods distribute randomly and have shorter length than the former, because the ultrasonic treatment in the ethanol solution made some nanorods broken from the substrate. In this regard, the specific surface area is higher in the grown ZnO arrays. To know the crystallogphy of the two kinds of products, the typical XRD characterization is shown in Fig. 1(d). All the diffraction peaks obtained in the range $30^\circ < 2\theta < 80^\circ$ can be indexed as the hexagonal wurtzite structured ZnO with lattice constants $a = 0.325$ nm and $c = 0.521$ nm, which are in good accordance with the data of standard XRD card (JCPDS 36-1451).

After immobilizing GO_x on two kinds of different ZnO/Au electrodes, the micrographs of GO_x functionalized surface of the transferred nanorods and the grown arrays are shown in Fig. 2 (a) and (b), respectively. These present that the transferred nanorods are interconnected with each other by GO_x while the grown ZnO arrays are covered by GO_x on their top ends. During the FESEM observation of two types of electrodes, the FESEM images are very difficult to focus, which can be attributed to a layer of coated protein film. The composition of the different ZnO electrodes modified with GO_x has been investigated through EDX spectrum analysis. The elemental analysis indicates that the modified ZnO nanorod electrodes consist of O, Zn, C, N and P, which confirms that the GO_x have been distributed equally on the modified electrode surface. A typical EDX spectrum is presented in Fig. 2(c).

Fig. 3 shows the CV characteristics of two kinds of GO_x/ZnO nanorod/Au electrodes in PBS in the absence and presence of 1 mM glucose. Both electrodes show only a small background current in PBS, whereas the CVs change remarkably with obvious increases of the oxidation current from 0.25 V of the transferred ZnO bioelectrode (in curve a) and 0.1 V of the grown ZnO bioeletrode (in curve c). This current increase is due to the oxidation of H_2O_2. The reactions can be described as follows:

$$\text{Glucose} + O_2^- \xrightarrow{GO_x} \text{Gluconolactone} + H_2O_2$$

$$H_2O_2 \rightarrow O_2 + 2H^+ + 2e^-$$

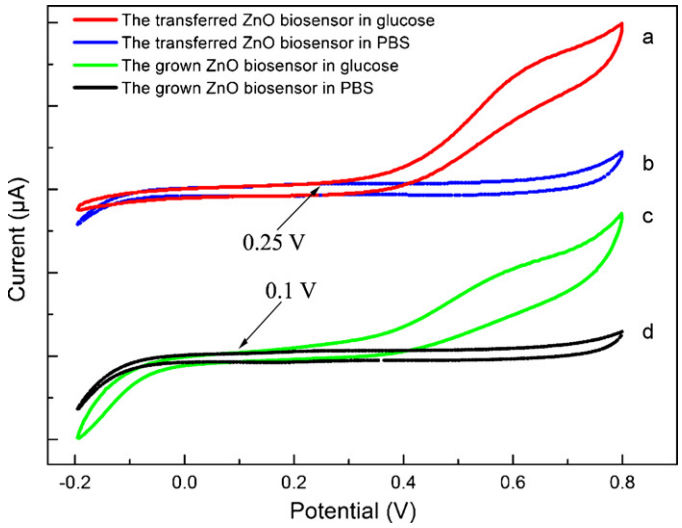

Fig. 3. CVs of GO_x modified the transferred ZnO nanorods and the grown ZnO arrays electrodes in the absence (curve b and d) and presence (curve a and c) of 1 mM glucose in PBS.

A glucose molecule gets oxidized by GO_x and releases two electrons, which lead to an increase in current. The glucose concentration can be determined by measuring the current derived from the electrochemical reaction of H_2O_2. The lower oxidation onset potential in the grown ZnO bioelectrode indicates that the oxidation occurrence is easier as compared to the transferred ZnO biosensor, because the well-aligned nanorod arrays supply the more direct electron transmission path [9].

In Fig. 4(a), the CV sweep curves of the GO_x modified grown ZnO bioelectrode in the glucose solutions with different concentrations (0, 3, 6, 10 and 15 mM) exhibit similar patterns with Fig. 3, and higher concentrations result in larger oxidation currents as expected in the same potential ranges. It can be clearly observed from the CV curves that the redox peak current increases with the increase of glucose concentration and saturates at the concentration between 10 and 15 mM, which is consistent with the previous report of 13 mM [8]. Fig. 4(b) represents CV curves with different scan rates (20, 40, 60, 80 and 100 mV/s) in 3 mM glucose for the kinetic and transport characteristics of GO_x/ZnO electrode. It can be found that the oxidation peak potential for H_2O_2 shifts positively with the increase of scan rates, suggesting a kinetic control over the redox at the active sites of the GO_x/ZnO electrode [21]. The anodic current increase is almost linear versus the square root of scan rate (correlation coefficient $R = 0.9951$) as shown in the inset of Fig. 4(b), indicating that a surface diffusion process controls the redox of H_2O_2 at the electrode [22].

For the detection of glucose, the amperometric response of the biosensors using the transferred and grown ZnO nanorods is shown in Fig. 5(a). With the successive addition of glucose concentration from 5 μM to 10 mM in 0.01 M PBS (pH 7.4) at an applied potential of 0.8 V, the oxidation current of the biosensors exhibits a sensitive and obvious increase, which is attributed to good catalytic behavior of GO_x/ZnO nanostructures [23]. The two types of sensors reach 90% of the steady state current in about 10 and 7 s, respectively, displaying a fast and direct electron exchange between GO_x and ZnO nanorods. The linear fitted sensitivity curves (the slope of current density versus concentration) of the ZnO nanorod biosensors prepared by two different methods are illustrated in Fig. 5(b). The sensitivities of the two biosensors are found to be 15.46 μA/cm^2/mM ($R = 0.9996$) and 23.43 μA/cm^2/mM ($R = 0.9952$), respectively. Relatively high sensitivity and fast response time of ZnO biosensor fabricated by Growth Method may be due to more GO_x immobilization on the well-aligned ZnO arrays structure, having the higher specific surface area and more direct electron communication path from ZnO nanostructures to the Au electrode, than the randomly distributed and stacked ZnO nanorods transferred. So, it results in more GO_x loading and leads to the enhancement of the electrocatalytic ability in the grown ZnO arrays biosensor.

Table 1 presents the comparative results of the key performance of the ZnO nanorod biosensors constructed by Coating Method and Growth Method. The detection limit (S/N = 3) and linear detection range of the grown ZnO biosensor are both better than those of the transferred one, which is in accord with their performance in sensitivities and response time (as shown in Fig. 5). These are attributed to the direct and fast electron conduction between the fixed GO_x and the Au electrode via vertical orientation ZnO nanorod arrays layer. The apparent Michaelis–Menten constant (K_M^{app}, a reflection of the enzymatic affinity) is calculated from the Lineweaver–Burk equation:

$$1/i = (K_M^{app}/i_{max})(1/C) + 1/i_{max}$$

(i: current, i_{max}: the maximum current, C: the glucose concentration)

The calculated result of the grown ZnO biosensor shows better affinity of the GO_x to glucose than that of the ZnO nail electrode

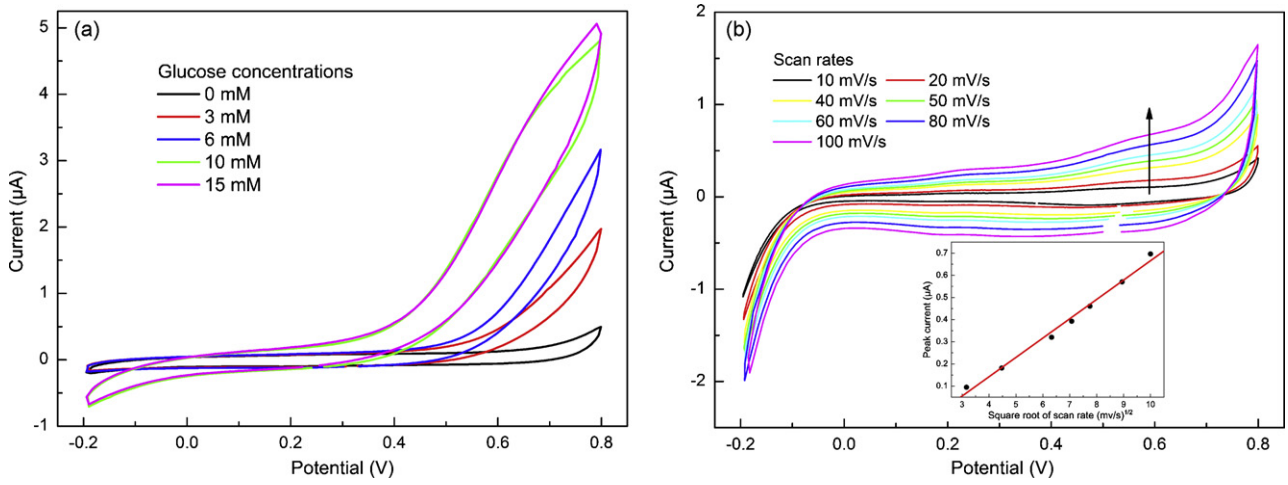

Fig. 4. CV curves of (a) the GO_x modified grown ZnO bioelectrode in different glucose solutions and (b) in 3 mM glucose at increased scan rates (the increase direction marked with the arrowhead). The inset of (b) shows the peak current as a linear function of scan rate.

Table 1
Comparison of the performance of the transferred ZnO biosensor and the grown ZnO biosensor.

ZnO nanorod biosensor	Sensitivity (μA/mM cm^2)	K_M^{app} (mM)	Detection limit (μM) S/N = 3	Response time (s)	Linear range (mM)
The transferred ZnO biosensor	15.46	3.097	50	~10	0.05–5.45
The grown ZnO biosensor	23.43	2.749	10	~7	0.01–5.9

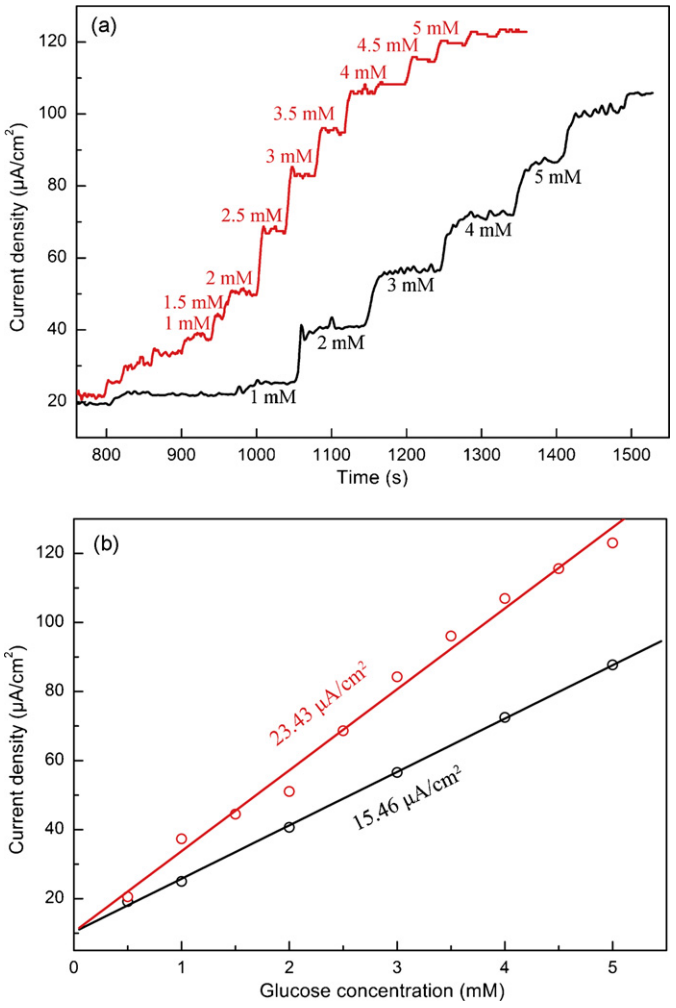

Fig. 5. (a) Amperometric response and (b) the corresponding calibration plot of the transferred biosensor (black lines) and the grown biosensor (red lines) with the successive addition of glucose (For interpretation of the references to color in this figure legend, the reader is referred to the web version of the article).

(14.7 mM) [24], the ZnO nanotube electrode (19 mM) [25] and many other electrodes modified with different methods [26–28]. It is worth noting that the K_M^{app} in the grown ZnO biosensor is also better than that in the transferred biosensor, because the GO_x is adsorbed on the ZnO arrays top ends, which is the Zn-terminated ZnO (0 0 0 1) polar surface of the ZnO nanorod arrays. The polar surface with chemically activity [29] may increase the surface activity of the enzyme.

The reproducibility of the grown ZnO biosensors was also examined by measuring the response towards 1 mM glucose in 25 mL 0.01 M PBS (pH 7.4). Three bioelectrodes, constructed independently, were characterized at identical conditions. The relative standard deviation (R.S.D.) is 2.4% for $n = 3$.

4. Conclusions

A comparative study of the technique of immobilizing nano-ZnO to construct biosensors has been achieved by transferring and growing ZnO nanorods. Our study shows that the nano-biosensor sensitivity not only depends on the nanomaterials morphology but also the immobilization technique of the nanostructures. An enhanced sensitivity of the grown ZnO biosensor is found to be 52% higher than that of the transferred ZnO biosensor. The two types of sensors achieve 90% of steady state current in around 10 and 7 s, respectively. The other properties, such as the K_M^{app}, detection limit and linear detection range, are also better in the grown ZnO biosensor. Thus the facile and more desirable approach of ZnO immobilization on the standard electrode for the biosensor fabrication has been determined. It is expected that the ZnO nanostructures grown directly will have more promising applications for enzymatic immobilization and signal transduction in the high performance biosensors.

Acknowledgements

Research was supported by the National Basic Research Program of China (Grant No. 2007CB936201), the Funds for International Cooperation and Exchange (Grant Nos. 50620120439, 2006DFB51000), the National Natural Science Foundation of China (Grant No. 50972011) and Beijing Novel Program (2008B19).

References

[1] Y. Masuda, K. Kato, Cryst. Growth Des. 8 (2008) 275.
[2] X.M. Zhang, M.Y. Lu, Y. Zhang, L.J. Chen, Z.L. Wang, Adv. Mater. 21 (2009) 2767.
[3] E. Topoglidis, A.E.G. Cass, B.O. Regan, J.R. Durrant, J. Electroanal. Chem. 517 (2001) 20.
[4] J. Zhao, D. Wu, J. Zhi, Bioelectrochemistry 75 (2009) 44.
[5] F.F. Zhang, X.L. Wang, S.Y. Ai, Z.D. Sun, Q. Wan, Z.Q. Zhu, Y.Z. Xian, L.T. Jin, K. Yamamoto, Anal. Chim. Acta 519 (2004) 155.
[6] Z. Dai, G. Shao, J. Hong, J. Bao, J. Shen, Biosens. Bioelectron. 24 (2009) 1286.
[7] A. Dorfman, N. Kumar, J. Hahm, Adv. Mater. 18 (2006) 2685.
[8] J.X. Wang, X.W. Sun, A. Wei, Y. Lei, X.P. Cai, C.M. Li, Z.L. Dong, Appl. Phys. Lett. 88 (2006) 233106.
[9] A. Wei, X.W. Sun, J.X. Wang, Y. Lei, X.P. Cai, C.M. Li, Z.L. Dong, W. Huang, Appl. Phys. Lett. 89 (2006) 123902.
[10] Y. Lei, X.Q. Yan, N. Luo, Y. Song, Y. Zhang, Colloids Surf. A 361 (2010) 169.
[11] X. Liu, Q. Hu, Q. Wu, W. Zhang, Z. Fang, Q. Xie, Colloids Surf. B 74 (2009) 154.
[12] J.P. Liu, C.X. Guo, C.M. Li, Y.Y. Li, Q.B. Chi, X.T. Huang, L. Liao, T. Yu, Electrochem. Commun. 11 (2009) 202.
[13] B.X. Gu, C.X. Xu, G.P. Zhu, S.Q. Liu, L.Y. Chen, X.S. Li, J. Phys. Chem. B 113 (2009) 377.
[14] A. Umar, M.M. Rahman, A. Al-Hajry, Y.B. Hahn, Talanta 78 (2009) 284.
[15] F. Battaglini, P.N. Bartlett, J.H. Wang, Anal. Chem. 72 (2000) 502.
[16] J.J. Burmeister, G.A. Gerhardt, Anal. Chem. 73 (2001) 1037.
[17] A.S.N. Murthy, J. Sharma, Anal. Chim. Acta 363 (1998) 215.
[18] F. Palmisano, R. Rizzi, D. Entonze, P.G. Zambonin, Biosens. Bioelectron. 15 (2000) 531.
[19] J.H. Yu, S.Q. Liu, H.X. Ju, Biosens. Bioelectron. 19 (2003) 401.
[20] Q.L. Liao, Y. Yang, L. Xia, J.J. Qi, Y. Zhang, Y.H. Huang, Z. Qin, Phys. Plasmas 15 (2008) 114505.
[21] X. Cao, W. Ning, L. Li, L. Guo, Sens. Actuators B 129 (2008) 268.
[22] L. Zhang, S. Dong, J. Electroanal. Chem. 568 (2004) 189.
[23] X.L. Zhu, I. Yuri, X. Gan, I. Suzuki, G.X. Li, Biosens. Bioelectron. 22 (2007) 1600.
[24] A. Umar, M.M. Rahman, S.H. Kim, Y.B. Hahn, J. Nanosci. Nanotechnol. 8 (2008) 3216.
[25] T. Kong, Y. Chen, Y. Ye, K. Zhang, Z. Wang, X. Wang, Sens. Actuators B 138 (2009) 344.
[26] X. Chen, J. Chen, C. Deng, C. Xiao, Y. Yang, Z. Nie, S. Yao, Talanta 76 (2008) 763.
[27] D. Shan, M. Zhu, H. Xue, S. Cosnier, Biosens. Bioelectron. 22 (2007) 1612.
[28] X. Chu, D. Duan, G. Shen, R. Yu, Talanta 71 (2007) 2040.
[29] Z.L. Wang, X.Y. Kong, J.M. Zuo, Phys. Rev. Lett. 91 (2003) 185502.